NASA TECHNICAL NOTE

NASA TN D-3545

NASA TN D-3545
c.1

LOAN COPY: RE
AFWL (WL
KIRTLAND AFB

TECH LIBRARY KAFB, NM
0130278

PRESSURE MEASUREMENTS ON RIGID MODEL OF BALLUTE DECELERATOR AT MACH NUMBERS FROM 0.56 TO 1.96

by Raymond A. Turk

Lewis Research Center

Cleveland, Ohio

NATIONAL AERONAUTICS AND SPACE ADMINISTRATION • WASHINGTON, D. C. • AUGUST 1966

TECH LIBRARY KAFB, NM
0130278

NASA TN D-3545

PRESSURE MEASUREMENTS ON RIGID MODEL OF BALLUTE DECELERATOR AT MACH NUMBERS FROM 0.56 TO 1.96

By Raymond A. Turk

Lewis Research Center
Cleveland, Ohio

NATIONAL AERONAUTICS AND SPACE ADMINISTRATION

For sale by the Clearinghouse for Federal Scientific and Technical Information
Springfield, Virginia 22151 – Price $1.00

PRESSURE MEASUREMENTS ON RIGID MODEL OF BALLUTE DECELERATOR AT MACH NUMBERS FROM 0.56 TO 1.96

by Raymond A. Turk

Lewis Research Center

SUMMARY

A pressure test of a 9-inch-diameter solid model of a ram-air-inflated conical balloon decelerator (ballute) was conducted in the Lewis 8- by 6-foot transonic wind tunnel over a Mach number range from 0.56 to 1.96 and a corresponding Reynolds number range from 3.60×10^6 to 4.90×10^6 per foot. Data were obtained with and without a cone-cylinder-flare forebody positioned between 0 and 16 forebody diameters forward of the decelerator. Drag coefficients were calculated from the pressure distributions.

In the subsonic regime the pressures and corresponding drag coefficients decrease slightly with increased separation distance. At supersonic speeds a discontinuous variation in pressure profile and, hence, drag coefficient was obtained with increased separation distance. At close distances the ballute caused divergence of the forebody wake, and the resulting pressures and drags were low. As the ballute was moved aft, the forebody wake converged and the measured pressure and corresponding drag were higher. At Mach numbers of 1.36 and greater, an intermediate range of separation distance was detected in which the type of forebody wake and, hence, pressure level and drag coefficient depended on the direction of ballute travel. For the cone-cylinder-flare forebody employed, a deployment to a distance of at least 4.2 forebody diameters was required to obtain maximum drag for Mach numbers of 1.36 and greater.

INTRODUCTION

The stabilization, deceleration, and structural requirements of recovery decelerators are particularly difficult to achieve at supersonic and hypersonic Mach numbers. The ballute (a ram-air-inflated conical balloon) concept has received attention as a possible solution in these high-speed ranges (ref. 1). Applications of the ballute presently being de-

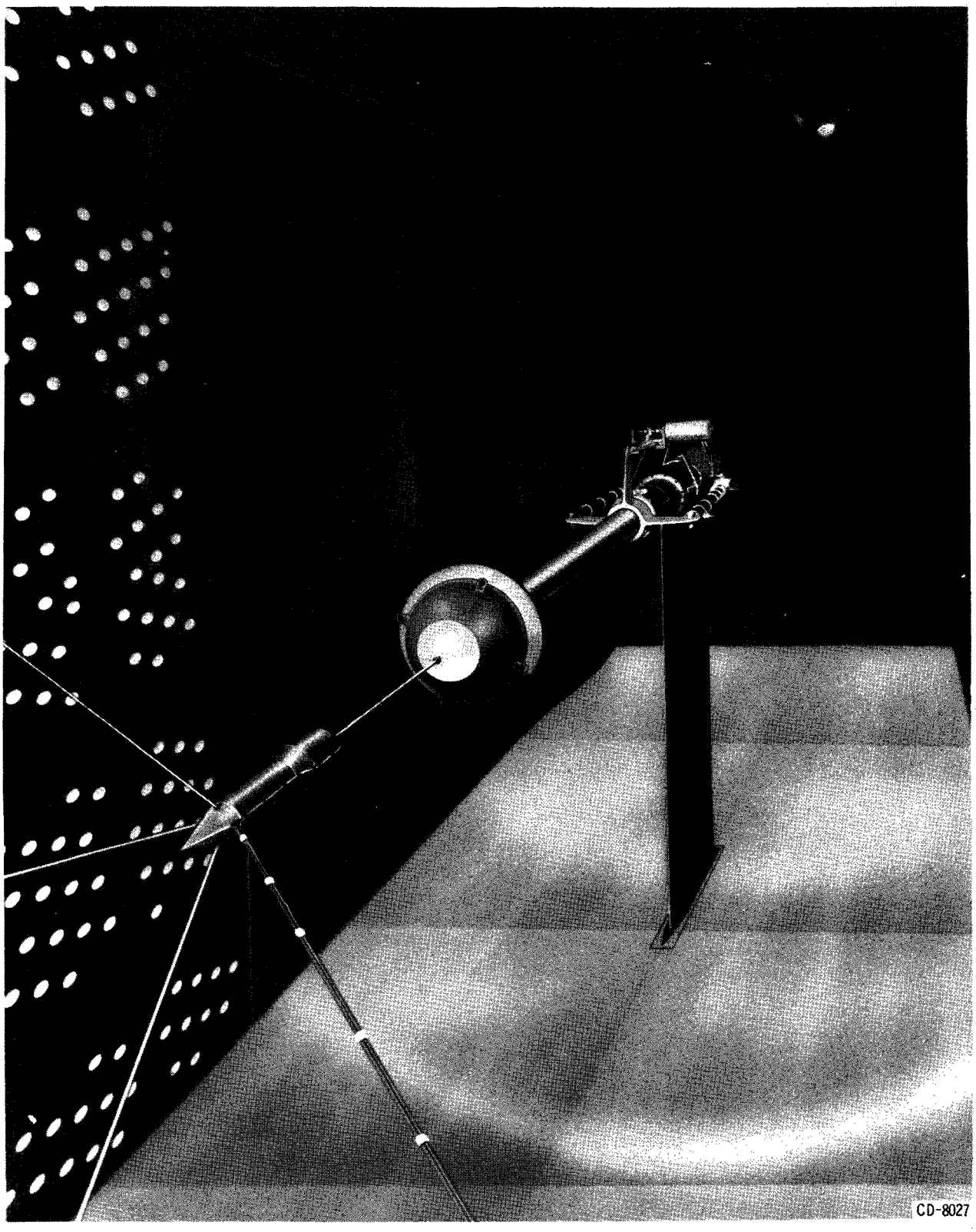

Figure 1. - Forebody and ballute model installed in wind tunnel.

veloped include (1) the initial deceleration and stabilization of personnel; (2) high speed, high altitude airplane ejection systems; (3) recoverable boost stages; and (4) returning space probes. In these applications, the ballute may remain deployed until subsonic speeds are reached and a conventional parachute may be utilized. To determine the structural requirements of a ballute design, details of local pressure loadings are required at all flight conditions. Pressure data have been obtained for a ballute similar to the one investigated herein in the speed range from Mach 1.5 to 6.0 (unpublished data), while drag data are available for a comparable shape at Mach 2.0 and above (refs. 2 and 3). A wind tunnel deployment and a stability test of a typical decelerator is reported in reference 4 for Mach numbers of 0.55, 1.73, and 1.92. Because transonic data are not reported in these references, the present investigation has been conducted in the Lewis 8- by 6-foot transonic wind tunnel to provide pressure and drag data at several Mach numbers in the speed regime from Mach 0.56 to 1.96.

The 9-inch-diameter solid model used in this investigation was instrumented with 60 static-pressure orifices to obtain distributions from which drag coefficients were computed. Since the pressure distribution over the surface of the ballute depends on its distance from its "payload", the distance between a cone-cylinder-flare forebody and the ballute was varied from 0 to 16 forebody diameters.

APPARATUS AND PROCEDURE

The complete ballute-forebody configuration, as installed in the Lewis 8- by 6-foot transonic wind tunnel, is shown in figure 1. The ballute was sting mounted, while the cone-cylinder-flare forebody was held by four wire-rope cables (attached to the tunnel walls, ceiling, and floor), and the tensioned line passing through the ballute and the sting. The distance between the ballute and the forebody was varied by moving the sting-mounted ballute fore and aft. Since the movable portion of the sting was limited to an 18-inch travel, the distance between the forebody and the ballute was varied from 0 to 36 inches by repositioning the forebody 18 inches forward in the wind tunnel. Details of the ballute-forebody model are presented in figure 2.

The forebody-to-ballute diameter ratio was 1 to 4, and the generalized shape of the forebody corresponded to that of a flight test vehicle. The ballute model incorporated the dummy air inlets and a burble fence. (Air inlets are normally used to inflate the ballute in flight.) The four ram-air inlets were located 90° apart in a plane perpendicular to the ballute centerline. The burble fence height of 10 percent of the basic ballute diameter has been shown by unpublished Goodyear Aircraft Corporation data to provide maximum drag without penalizing stability.

Ballute base pressure data were obtained with sting diameters of 25, 33, and 44 percent of the ballute diameter. These variations in sting diameter, shown in figure 2, were

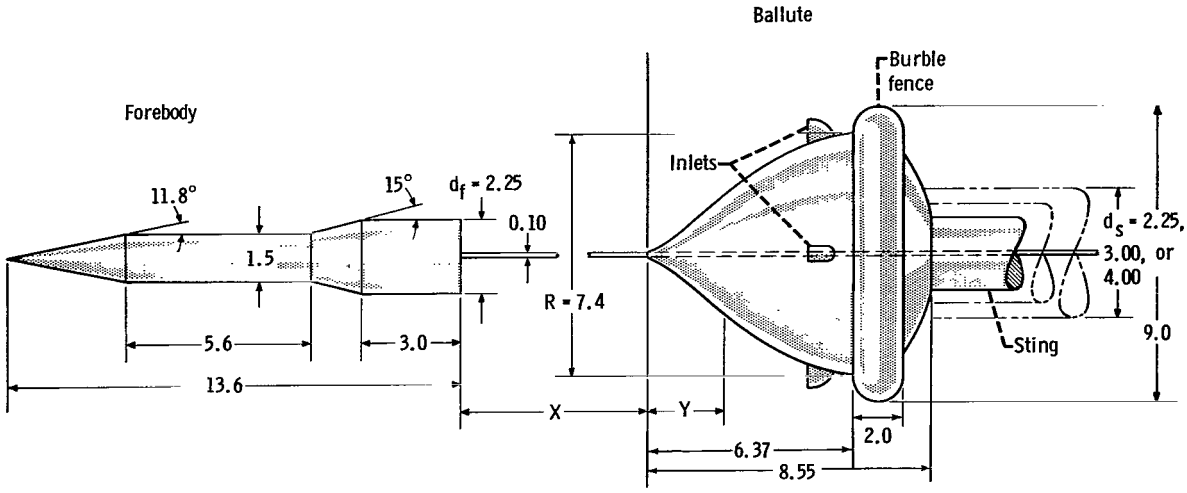

Figure 2. - Schematic diagram of forebody and ballute model. (All dimensions in inches.)

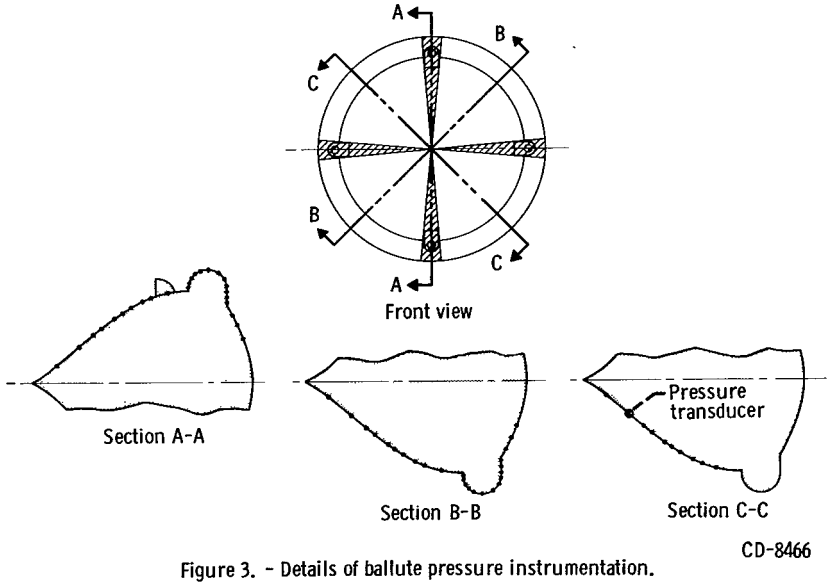

Figure 3. - Details of ballute pressure instrumentation.

achieved by adding shrouds to the basic 2.25-inch sting. The effect of the sting diameter on ballute base pressure was obtained so that the flight base pressure without sting effects, could be estimated by extrapolating the observed effect.

Details of the ballute pressure instrumentation are presented in figure 3. The instrumentation consisted of two complete rows of pressure orifices, one along a ray including a ram-air inlet (section A-A) and one along a ray with no inlet (section B-B), and one partial row (section C-C) duplicating the front half of section B-B. Pressure taps in each row were located at the radial centroids of equal-area projections normal to the ballute axis. Overall ballute drag was calculated by assuming that the average pressure from row A-A acted on 10 percent of the total projected area (the projected areas subtended by the width of the simulated inlets) and that the average pressures from rows B-B and C-C acted on the remaining 90 percent (fig. 3). Drag coefficients presented in the

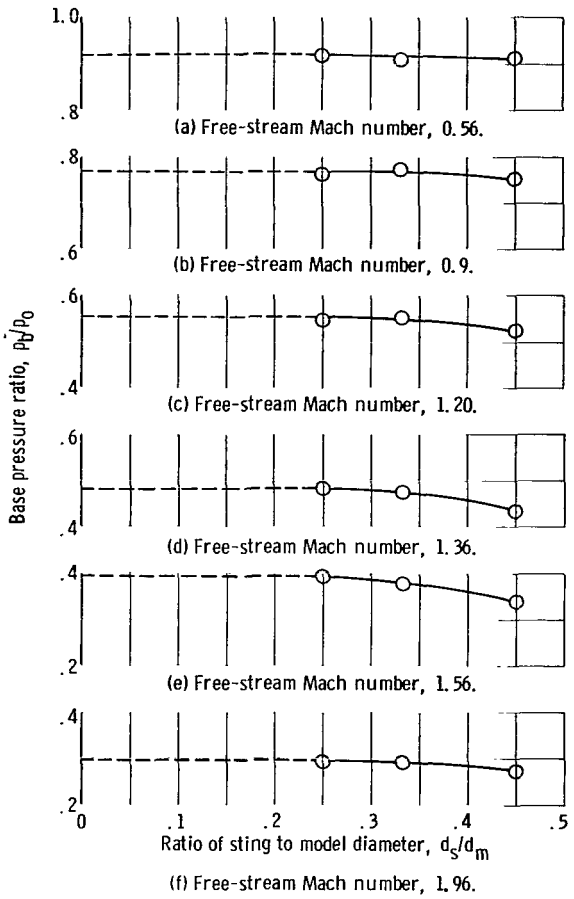

Figure 4. - Effect of sting-model diameter ratio on base pressure ratio.

figures are references to the maximum ballute area without burble fence.

The actual testing of the ballute-forebody combination was conducted in two phases. In the preliminary phase, the ballute was extended and retracted in a continuous sweep. Although the ballute is not retracted during flight deployments, it was retracted in the present testing as a matter of completeness. The ballute pressure was sensed by a pressure transducer (fig. 3, row C-C) and was recorded on an X-Y plotter. This pressure variation was used to select specific ballute extensions at which steady-state data were to be recorded. Ballute pressure distributions, measured without the forebody, and the collection of other steady-state data constituted the main phase of this investigation.

RESULTS AND DISCUSSION

To obtain drag coefficients that would be comparable to free flight, the sting effect encountered in wind tunnel testing has to be considered. Preliminary tests with the three different sting diameters indicated that the base pressure ratio was fairly insensitive to sting-to-model diameter ratio at values less than 0.33 (fig. 4). All testing was, therefore, conducted with the smallest sting, and the average measured base pressures were considered to act over the entire projected base area.

The variation of ballute drag coefficient C_D with free-stream Mach number M_0 (comparable to the short-body C_D curves of ref. 3) is presented in figure 5 for selected values of separation-distance ratio x/d (fig. 2). (Symbols are defined in the appendix.) The rate of change of C_D with Mach number is greatest below $M_0 = 1.10$. Depending on the separation distance, the maximum drag occurred between Mach 1.2 and 1.45. The decrease in the drag coefficient at higher speeds is almost linear. At supersonic Mach numbers, a minimum value of drag was obtained at the separation-distance ratio x/d = 2, and a maximum value was obtained without the forebody. At an intermediate separation-distance ratio of 6, nearly maximum drag was obtained above Mach 1.40. At Mach num-

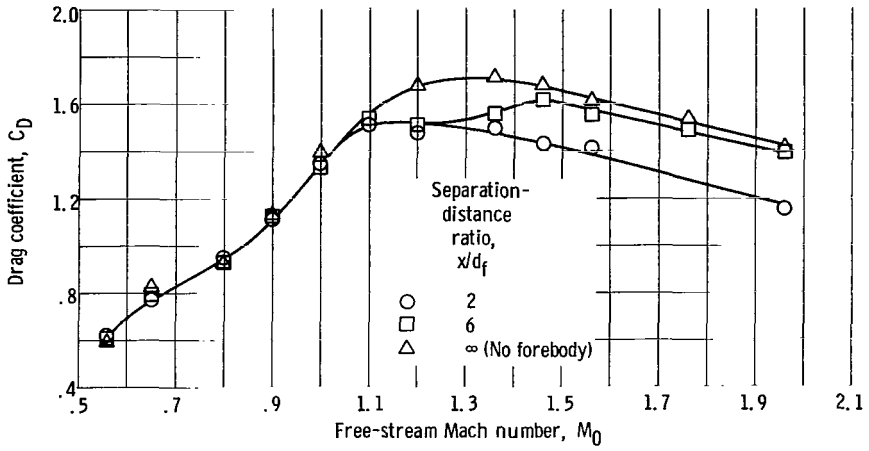

Figure 5. - Variation of ballute drag coefficient with Mach number for three ballute-forebody separations.

bers less than 1. 10, separation distance had little effect on the ballute drag coefficient.

The detailed effects of ballute-forebody separation on drag coefficient are shown in figure 6 for specific values of Mach number. In the subsonic range (figs. 6(a) and (b)), the drag coefficient varied linearly with separation distance. The negative slopes of the curves can be attributed to a slight but persistent decrease in ballute frontal pressures. At transonic speeds (fig. 6(c)) the change was no longer linear, and at supersonic speeds (figs. 6(d) to (f)) an abrupt change in C_D was detected between separations of 2. 1 and 4. 2 forebody diameters. The change in C_D occurs (fig. 6(f)) at a larger x/d for an increasing ballute-forebody separation than for a decreasing separation. This effect is the hysteresis phenomenon observed in previous studies. When the ballute is beyond the hysteresis region, it is also beyond the point at which the forebody wake converges and, hence, out of the low energy flow of the initially divergent wake. This may be considered a critical separation beyond which the ballute would have to be deployed to achieve maximum drag. Figure 7 shows that the ballute with the diameter ratio of 4 would have to be deployed to a distance of at least 4. 2 forebody diameters to maintain maximum drag for Mach numbers of 1. 36 to 1. 96.

Figures 8 to 10 show the variation of local pressure (in coefficient form) along the ballute surface for typical Mach numbers and separation distances. Pressure measurements for both the ray without a ram-air inlet (representative of 90 percent of the ballute surface) and the ray intersecting the ram-air inlet (representative of the remaining 10 percent of the ballute surface) are presented since both entered into the calculation of the overall ballute drag coefficient. In figure 8 the same general shape is maintained throughout the Mach number range, since the ballute-forebody separation of 6 forebody diameters places the ballute downstream of most of the forebody wake effects. The one change that is noticed occurs at supersonic speeds near the tip of the ballute, where the low energy flow related to the wake of the forebody causes the lower pressures which are shown in

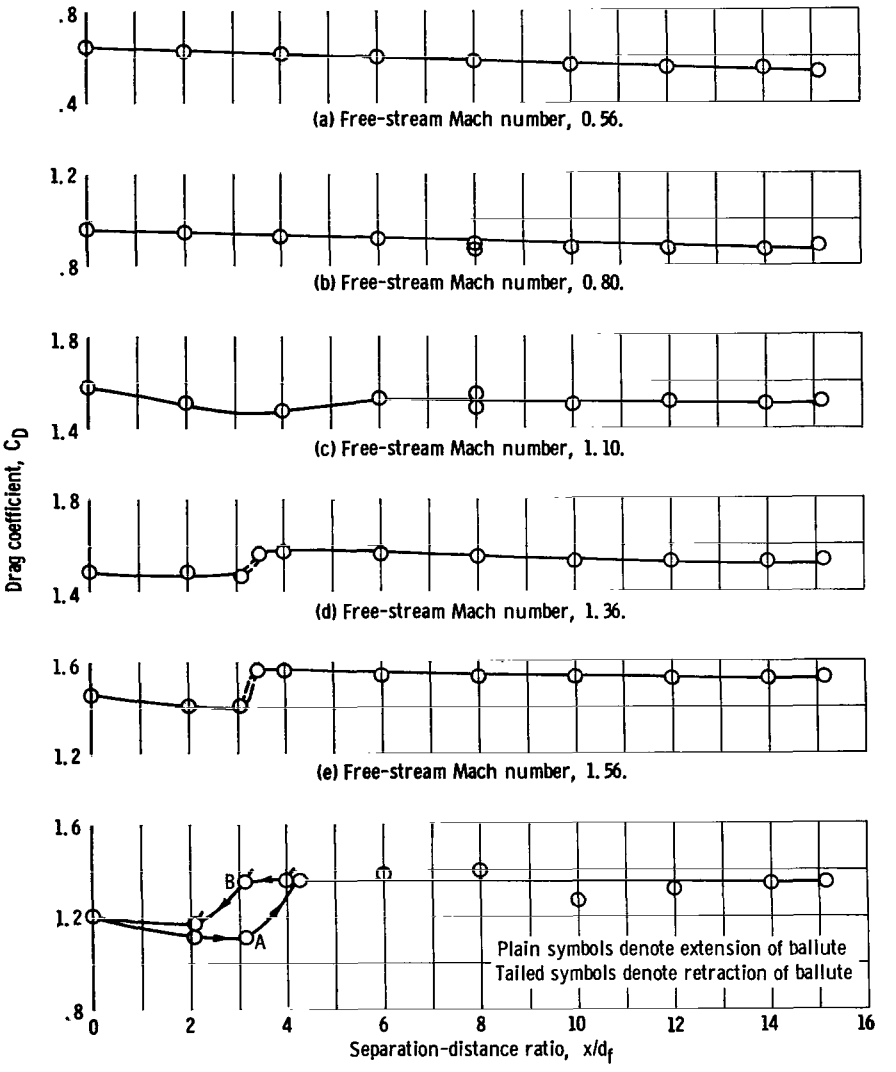

Figure 6. - Effect of ballute-forebody separation on ballute drag coefficient.

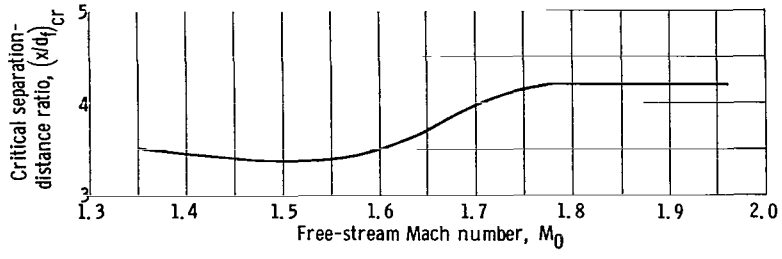

Figure 7. - Variation of critical ballute-forebody separation with Mach number.

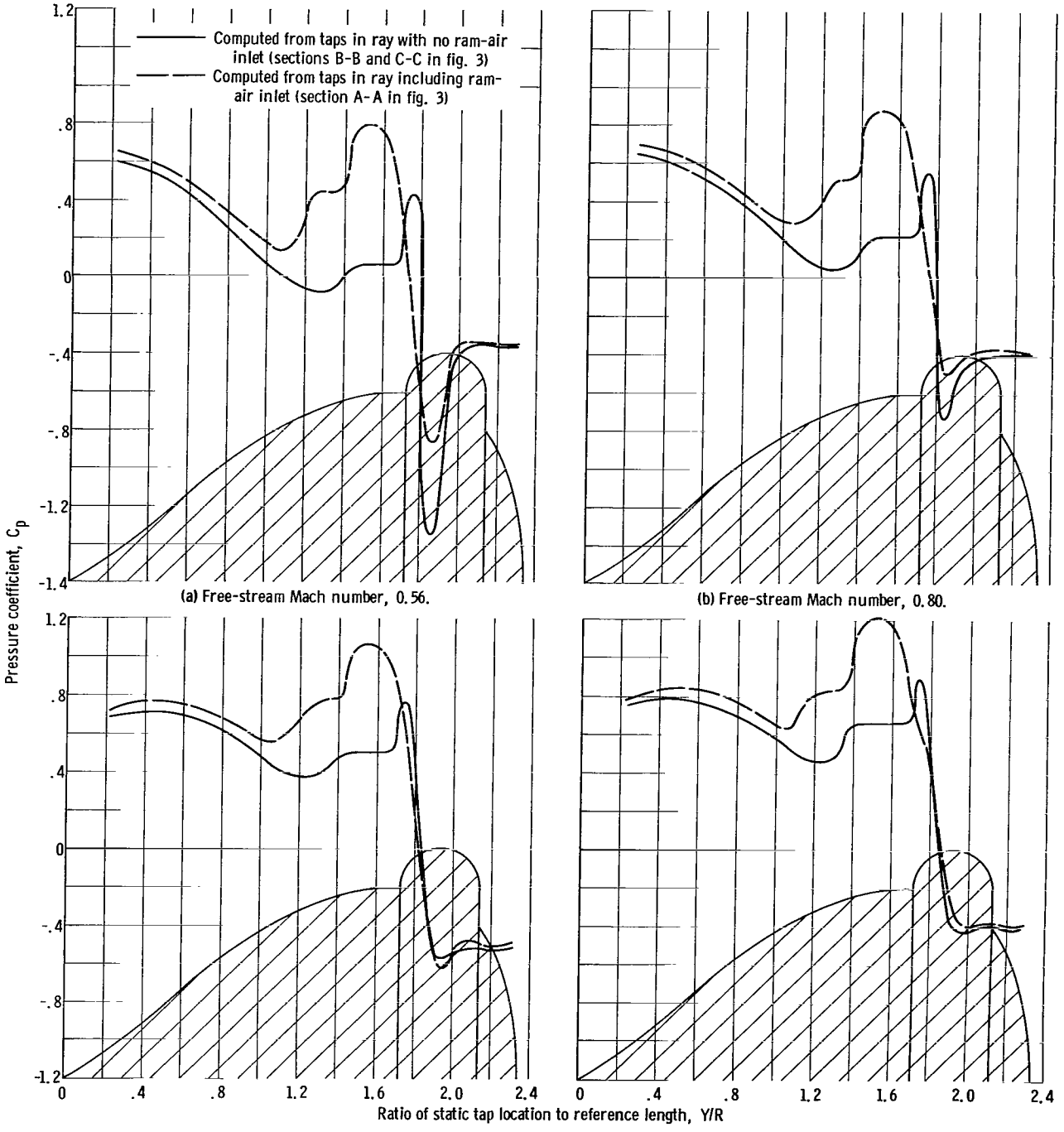

Figure 8. - Effect of free-stream Mach number on ballute pressure distribution for constant ballute-forebody separation of 6 forebody diameters.

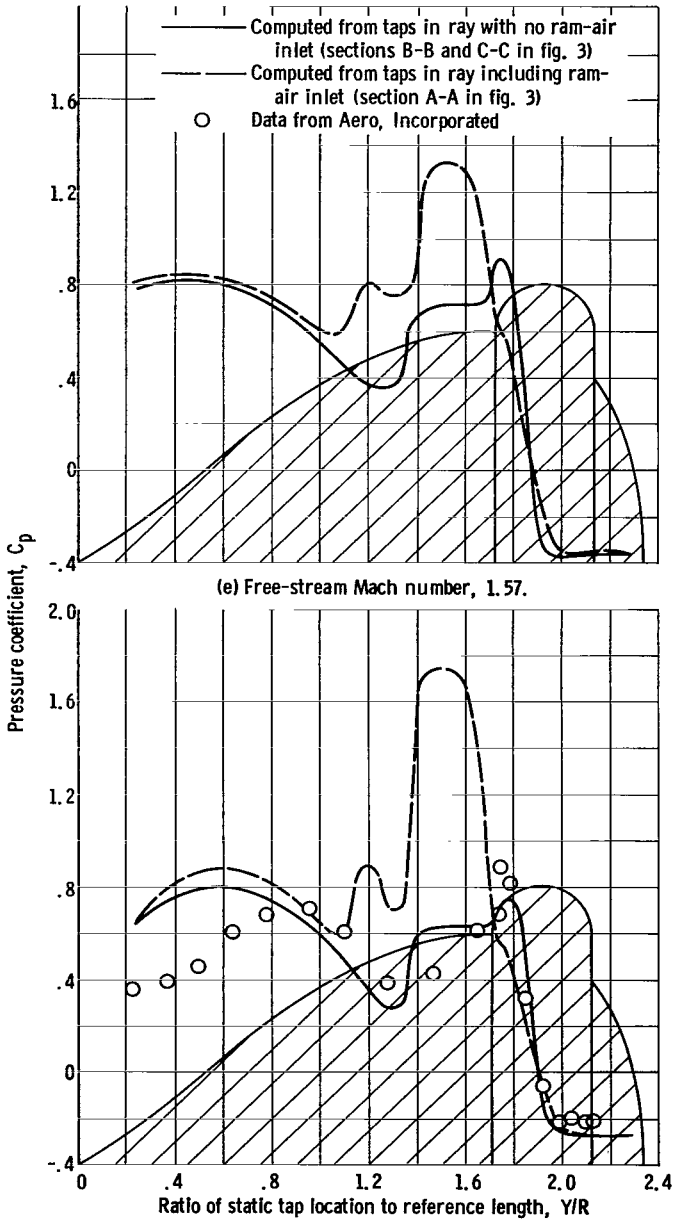

(e) Free-stream Mach number, 1.57.

(f) Free-stream Mach number, 1.96.

Figure 8. - Concluded.

figure 8. These pressures in turn result in drags lower than those recorded without the forebody (fig. 5), where no regions of subsonic flow exist. An overall increase in pressure coefficient with an increase in Mach number is expected for the short blunt shape of the ballute. The pressures measured over the base of the ballute are fairly constant at each test condition. The Mach 1.96, $x/d = 6$ data of figure 8(f) are compared to Mach 2.0, $x/d = 6$ results (obtained by Aero, Incorporated). The lower pressures of the cited data for $Y/R < 1.0$ may be attributed to the 0.50- to 0.75-inch-diameter three-piece telescoping actuator used to support and move the forebody during the previous study. Other variations in the compared data are possibly due to the geometrical differences in the forebodies of the respective tests. A thorough analysis of the flow fields of each configuration and test condition is beyond the scope of this report.

Figure 9 shows the pressure distribution along the ballute surface at Mach 1.36 over a range of separation distances. At an x/d of 2.04 the ballute is in the diverging wake of the forebody. The lower pressures along the first half of the ballute face indicate the portion affected by the diverging wake of the relatively small diameter forebody. When the ballute is aft of the point at which the forebody wake converges (fig. 9(b)), only the initial portion of the surface experiences the lower energy flow, as discussed in the

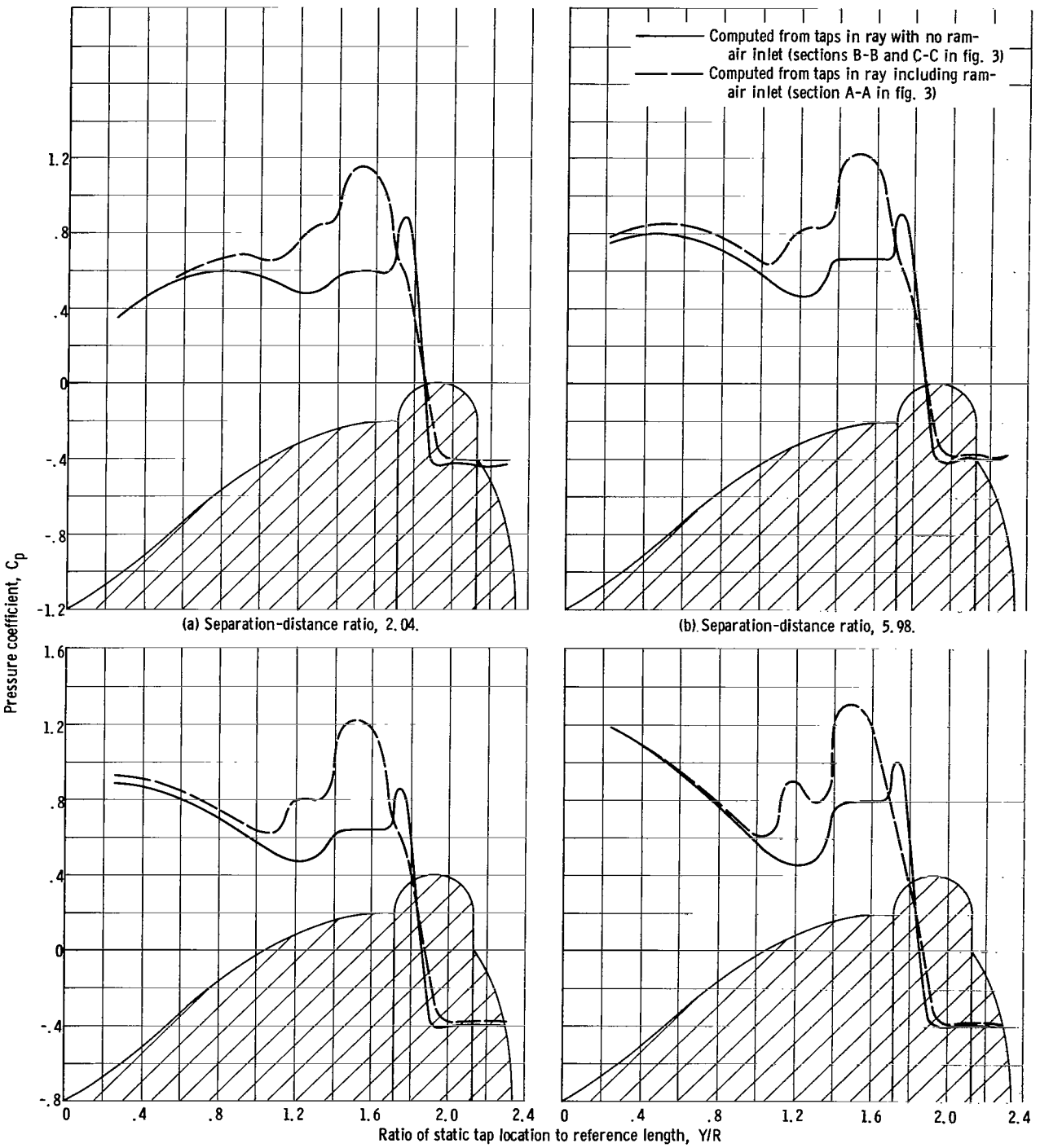

(a) Separation-distance ratio, 2.04.

(b) Separation-distance ratio, 5.98.

(c) Separation-distance ratio, 15.15.

(d) Separation-distance ratio, ∞ (no forebody).

Figure 9. - Typical variations of ballute pressure distributions with ballute-forebody separation. Free-stream Mach number, 1.36.

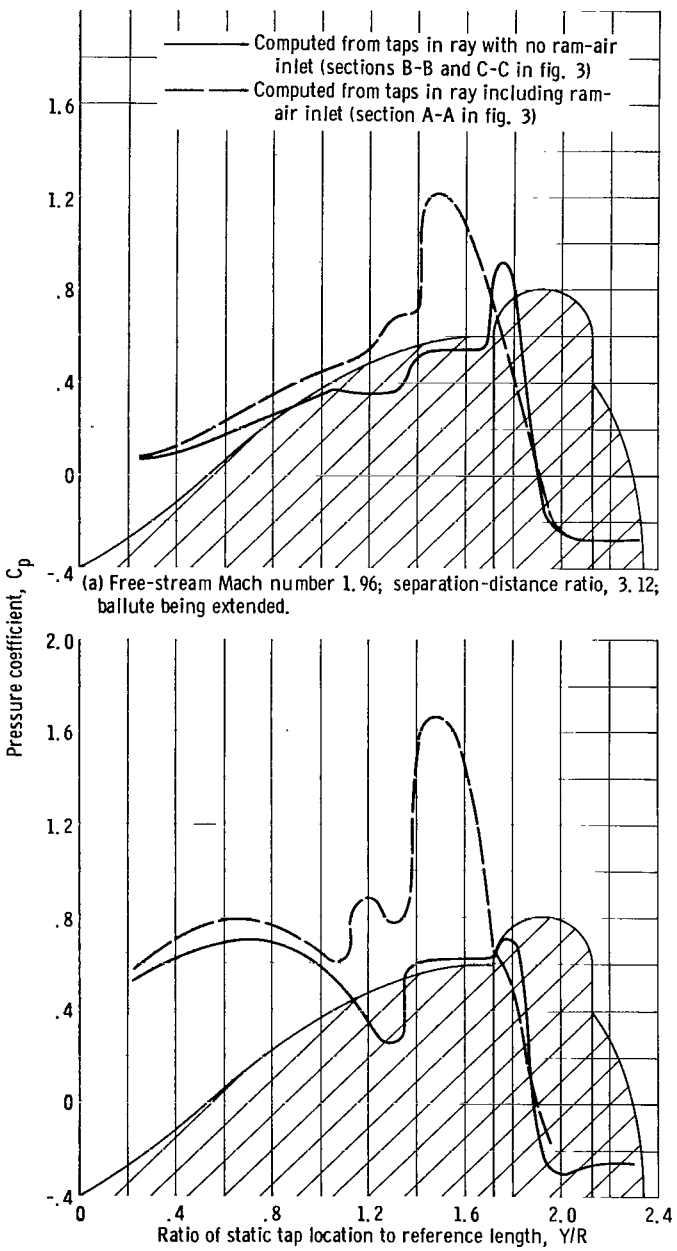

(a) Free-stream Mach number 1.96; separation-distance ratio, 3.12; ballute being extended.

(b) Free-stream Mach number, 1.96; separation-distance ratio, 3.12; ballute being retracted.

Figure 10. - Typical variation of pressure distributions for constant ballute-forebody separation in hysteresis region.

preceding paragraph. Moving the ballute farther aft to an x/d of 15.15 had little effect on the overall pressure distribution. The pressure distribution for the ballute alone (fig. 9(d)) is presented as an ideal profile where the entire decelerator is exposed to supersonic flow. The general increase in pressures is probably due to the different shock patterns developed when the ballute is out of the wake of the forebody.

Figure 10 presents the pressure distributions for a $M_0 = 1.96$, x/d = 3.12 condition. The difference in the profiles of figures 10(a) and (b) shows that, although the ballute is at a specific deployment position, it can experience two distinct types of flow, depending on its direction of travel. Figure 10(a) (corresponding to point A of fig. 6(f)) is characteristic of the pressure distribution detected when the ballute is extended from a separation distance of zero and is in the diverging wake of the forebody. Pressure levels and the corresponding drag are relatively low. When the ballute is retracted to an x/d of 3.12 (point B of fig. 6(f)), the pressure profile is typical of a location aft of a converging forebody wake and the overall pressures and drag are higher.

SUMMARY OF RESULTS

Pressure distribution data were obtained with a solid model simulating a

ram-air-inflated ballute decelerator over a Mach number range from 0.56 to 1.96 and for ballute-forebody separations from 0 to 16 forebody diameters. Surface pressures were measured with and without the cone-cylinder-flare forebody and were used to compute drags and drag coefficients. The following observations were made:

1. In the subsonic speed range, the general level and distribution of pressures and the corresponding drag coefficients decrease slightly with increased separation distance.

2. In the supersonic speed range, the pressure distributions and computed drag coefficients showed a definite dependence on separation distance. At close distances (between $x/d = 0$ and $x/d = 3$, where x is the ballute-forebody separation distance and d_f is the forebody base diameter) the ballute was in the diverging wake of the forebody and both the resulting pressures and drag were relatively low. At separation distances greater than 4.2 the ballute was aft of the converged forebody wake and pressures and drag were higher. A hysteresis effect was observed at Mach numbers of 1.36 and greater, since the direction of ballute travel also affected the position at which the forebody wake changed from a convergent to a divergent shape. This effect became increasingly apparent as Mach number increased for separations between 2.1 and 4.2 forebody diameters.

3. For the forebody studied, a ballute-forebody separation greater than 4.2 would be required for maximum decelerator drag for Mach numbers of 1.36 to 1.96.

Lewis Research Center,
National Aeronautics and Space Administration,
Cleveland, Ohio, March 28, 1966.

APPENDIX - SYMBOLS

A_{ref} reference area based on maximum ballute diameter without burble fence of 7.4 in. (see fig. 2), 0.299 sq ft

A_t total projected area based on maximum ballute diameter, 0.442 sq ft

C_D drag coefficient, $D/q_0 A_{ref}$

C_P pressure coefficient, $(p_\ell - p_0)/q_0$

D drag, $(\overline{p}_i - \overline{p}_j) A_t$, lb

d_f forebody base diameter (see fig. 2), 2.25 in.

d_m maximum ballute diameter (see fig. 2), 9.0 in.

d_s sting diameter (see fig. 2), 2.25 in. unless noted

M_0 free-stream Mach number

p static pressure, lb/sq ft

$\overline{p}_i$ average local pressure measured forward of maximum ballute diameter, lb/sq ft

$\overline{p}_j$ average local pressure measured aft of maximum ballute diameter, lb/sq ft

q dynamic pressure, lb/sq ft

R radius of ballute without burble fence, reference length, (see fig. 2), 3.7 in.

x ballute-forebody separation distance (see fig. 2), in.

Y static tap location aft of ballute tip measured along model centerline (see fig. 2), in.

Subscripts:

b base

cr critical

ℓ local

0 free-stream conditions

REFERENCES

1. Maynard, Julian D.: Aerodynamics of Decelerators at Supersonic Speeds. Proc. Recovery of Space Vehicles Symposium, Aug. 31-Sept. 1, 1960, pp. 48-54.
2. McShera, John T., Jr.: Aerodynamic Drag and Stability Characteristics of Towed Inflatable Decelerators at Supersonic Speeds. NASA TN D-1601, 1963.
3. Hoermer, Sighard F.: Fluid Dynamic Drag. S. F. Hoermer, pub., cc. 1965.
4. White, Warren E.; and Riddle, Charles D.: An Investigation of the Deployment Characteristics and Drag Effectiveness of the Gemini Personnel Decelerator at Subsonic and Supersonic Speeds, Phase II. Rept. No. AEDC-TDR-63-255, Aro, Inc., Dec. 1963.

"The aeronautical and space activities of the United States shall be conducted so as to contribute . . . to the expansion of human knowledge of phenomena in the atmosphere and space. The Administration shall provide for the widest practicable and appropriate dissemination of information concerning its activities and the results thereof."

—NATIONAL AERONAUTICS AND SPACE ACT OF 1958

NASA SCIENTIFIC AND TECHNICAL PUBLICATIONS

TECHNICAL REPORTS: Scientific and technical information considered important, complete, and a lasting contribution to existing knowledge.

TECHNICAL NOTES: Information less broad in scope but nevertheless of importance as a contribution to existing knowledge.

TECHNICAL MEMORANDUMS: Information receiving limited distribution because of preliminary data, security classification, or other reasons.

CONTRACTOR REPORTS: Technical information generated in connection with a NASA contract or grant and released under NASA auspices.

TECHNICAL TRANSLATIONS: Information published in a foreign language considered to merit NASA distribution in English.

TECHNICAL REPRINTS: Information derived from NASA activities and initially published in the form of journal articles.

SPECIAL PUBLICATIONS: Information derived from or of value to NASA activities but not necessarily reporting the results of individual NASA-programmed scientific efforts. Publications include conference proceedings, monographs, data compilations, handbooks, sourcebooks, and special bibliographies.

Details on the availability of these publications may be obtained from:

SCIENTIFIC AND TECHNICAL INFORMATION DIVISION

NATIONAL AERONAUTICS AND SPACE ADMINISTRATION

Washington, D.C. 20546